

# Fundamental flow problems considering non-Newtonian hyperbolic tangent fluid with Navier slip: Homotopy analysis method

L. Tlau<sup>a,\*</sup>

<sup>a</sup>*Department of Mathematics, National Institute of Technology Mizoram, Aizawl 796012, India*

Received 6 July 2020; accepted 16 October 2020

---

## Abstract

The presented research article deals with the classical fundamental flows (Poiseuille and Couette) of an incompressible hyperbolic tangent fluid while considering the Navier slip at the walls. The governing equations are solved using the homotopy analysis method. The velocity expressions are obtained for each problem and the effect of the flow parameters are discussed while being supplemented by graphical displays. Increasing the slip parameter reduces the fluid velocity for both problems, respectively. An increase in the Weissenberg number shows that skin friction at the lower wall reduces. This shows that a dominant elastic force is crucial in reducing the skin friction. © 2020 University of West Bohemia. All rights reserved.

*Keywords:* hyperbolic tangent fluid, Couette flow, Poiseuille flow, Navier slip

---

## 1. Introduction

The contact point between a fluid and a solid surface poses interesting questions. Many investigations have been undertaken and yet plenty of questions remain unanswered. As in the case of many engineering problem approximations, no-slip condition at the contact point of a moving fluid and a solid boundary has been found to be impractical for many cases [27]. Hence, the Navier slip at the contact point of fluid and solid body have been used prominently for theoretical studies as it has been found to be more realistic in view of real life applications. The Navier slip condition shows that the velocity of the moving fluid is directly proportional to the shear stress at the contact point of the fluid and solid boundary. The constant of proportionality is called the slip length. The non-dimensional slip parameter have been observed to be related to the direction of the fluid flow [24]. Usage of non-Newtonian fluids in industrial settings have slowly gained prominence in the last few decades. The hyperbolic tangent fluid is a subclass of non-Newtonian fluid which offers a shear thinning behavior and plays an important role in chemical engineering applications. Fluids such as paints, blood, ketchup or cream are examples of tangent hyperbolic fluid. Compared to other types of non-Newtonian fluids, the tangent hyperbolic fluid is rather simple, easily computable and is physically robust. Investigations in the present literature have reported few results of Navier slip on hyperbolic tangent fluid flows. However, the flow regimes have mostly been based on peristaltic flows [11–13], while a few others have been on flows over flat surfaces [4, 7, 21]. Skin friction has been reported to be diminished when the power law index was increased [15]. While the Weissenberg number has been reported to increase the hyperbolic tangent fluid flow in a channel [3]. Non-Newtonian fluid flow problems poses highly

---

\*Corresponding author. Tel.: +919 862 721 036, e-mail: puiatlau0610@gmail.com.  
<https://doi.org/10.24132/acm.2020.628>

nonlinear differential equations and must be tackled intricately. The homotopy analysis method (HAM) [17, 19] has been developed for such purposes. The HAM has been used successfully to solve numerous types of equations [1, 2, 9, 18, 20, 23, 28, 29, 31] and has been found to be extremely reliable [6, 26].

In light of the presented literature review, the gap in the literature of Poiseuille and Couette flows of a tangent hyperbolic fluid is studied in the presented article. The Navier slip effect is assumed at the walls of the channel. For the Poiseuille flow, the flow is pressure driven and the walls are assumed to be stationary. For the case of the Couette flow, the flow is pressure driven while also being supplemented by the movement of the upper channel wall in the direction of the flow. The article is divided into several sections each focusing on a different aspect of the investigation. The second section focuses on the mathematical formulation of the tangent hyperbolic fluid in the Cartesian coordinates for the present problem in consideration. In the third section, the homotopy analysis method is introduced which is used to solve the nonlinear differential equation governing the flow. Section 4 is dedicated to the discussion of the results which are obtained in the previous section. The concluding remarks of the study are presented in the last section.

## 2. Governing equation formulation

Let us consider an incompressible non-Newtonian hyperbolic tangent fluid. A hyperbolic tangent fluid is a four constant fluid model describing the shear thinning effects of the fluid. The Cauchy stress tensor for the non-Newtonian hyperbolic tangent fluid can be written as [14, 25]

$$\tau = [\kappa_\infty + (\kappa_0 + \kappa_\infty) \tanh^n(\Gamma\beta)]\beta, \tag{1}$$

where  $\tau$  is the extra stress tensor,  $\kappa_\infty$  is the shear rate viscosity at infinity,  $\kappa_0$  is the initial shear rate viscosity,  $\Gamma$  is the time dependent material constant,  $n$  is the power law index and  $\beta$  is the shear rate. As the hyperbolic tangent fluid is a shear thinning fluid, we can conclude that  $\kappa_\infty = 0$  and  $\Gamma\beta \ll 1$  such that  $\tanh(\Gamma\beta) \approx (\Gamma\beta)$ . Thus, the Cauchy stress tensor (1) takes the form

$$\tau = \kappa_0[(\Gamma\beta)^n]\beta = \kappa_0[(1 + \Gamma\beta - 1)^n]\beta = \kappa_0[1 + n(\Gamma\beta - 1)]\beta. \tag{2}$$

For a laminar, fully developed fluid flow, the velocity field is reduced to  $\mathbf{U} = (u(y), 0, 0)$ . In the absence of external body forces and a constant pressure gradient acting along the flow direction, the momentum equation of a hyperbolic tangent fluid can be written as [32]

$$\mu_f(1 - s) \frac{d^2u}{dy^2} + \sqrt{2}s\mu_f\Gamma \left( \frac{du}{dy} \right) \frac{d^2u}{dy^2} = \frac{dp}{dx}. \tag{3}$$

Introducing the non-dimensional terms as

$$U = \frac{u}{U_0}, \quad Y = \frac{y}{L}, \quad \text{We} = \frac{\Gamma U_0}{L}, \quad P = -\frac{L^2}{U_0\mu_f} \frac{dp}{dx}, \tag{4}$$

we have

$$(1 - s) \frac{d^2U}{dY^2} + \sqrt{2}s\text{We} \left( \frac{dU}{dY} \right) \frac{d^2U}{dY^2} + P = 0, \tag{5}$$

where  $s$  is the power law index,  $\text{We}$  is the Weissenberg number, and  $P$  is the dimensionless pressure gradient.

An important aspect of fluid flows is the skin friction at the fluid–solid interface. The skin friction is the resistance exerted by a solid body on a moving fluid. For the present analysis, the skin friction offered by the channel wall on the flowing hyperbolic tangent fluid is expressed in the non-dimensional form as

$$Cf = U'(-1). \tag{6}$$

### 2.1. Poiseuille flow

For the Poiseuille fluid flow, consider the hyperbolic tangent fluid flowing between two infinitely long parallel horizontal plates which are at a distance  $2L$  apart. The lower wall is taken to be at  $y = -L$ , while the upper wall is at  $y = L$ . The Navier slip at the walls are also considered. Thus, the conditions of the velocity at the walls of the channel can be written as [8]

$$u(-L) = -\alpha \left. \frac{du}{dy} \right|_{y=-L}, \quad u(L) = \alpha \left. \frac{du}{dy} \right|_{y=L}. \tag{7}$$

Invoking (4), we have

$$U(-1) = -\gamma \left. \frac{dU}{dY} \right|_{Y=-1}, \quad U(1) = \gamma \left. \frac{dU}{dY} \right|_{Y=1}, \tag{8}$$

where  $\gamma = \alpha/L$  is the dimensionless slip parameter.

### 2.2. Couette flow

For the Couette flow, again consider the hyperbolic tangent fluid flowing between two infinitely long horizontal plates kept at a distance  $2L$  apart such that the upper wall is at  $y = L$  and the lower wall is at  $y = -L$ . For the general Couette flows, the fluid flow is aided by the movement of the upper plate in the direction of the flow. Hence, considering the existence of the Navier slip, the condition of the velocity at the lower wall and upper moving wall of the channel can be described as [8]

$$u(-L) = -\alpha \left. \frac{du}{dy} \right|_{y=-L}, \quad u(L) = \alpha \left. \frac{du}{dy} \right|_{y=L} + u_w. \tag{9}$$

Invoking (4), we have

$$U(-1) = -\gamma \left. \frac{dU}{dY} \right|_{Y=-1}, \quad U(1) = \gamma \left. \frac{dU}{dY} \right|_{Y=1} + U_w, \tag{10}$$

where  $U_w = u_w/U_0$  is the wall velocity parameter.

The general expression of the fluid flow velocity can be obtained by taking  $s = 0$  and  $\gamma = 0$  and integrating (5) for both cases.

## 3. Analytical solution by HAM

We define a set of base functions as

$$\{Y^n | n \geq 0\} \tag{11}$$

to define the velocity expression in the form

$$U(Y) = \sum_{n=0}^{\infty} C_n Y^n, \tag{12}$$

where  $C_n$  is a coefficient. Using the boundary conditions for each problem, the initial guess approximations [18] are chosen as

$$U_0(Y) = \begin{cases} 0 & \text{for the Poiseuille flow,} \\ \left(1 + \frac{Y}{1-\gamma}\right) \frac{U_w}{2} & \text{for the Couette flow.} \end{cases} \quad (13)$$

The linear operator

$$\frac{d^2}{dY^2} = L \quad (14)$$

such that

$$L[K_1 + K_2 Y] = 0, \quad (15)$$

where  $K_1$  and  $K_2$  are unknown constants. Let  $h$  be the convergence controlling parameter and  $q \in [0, 1]$  be the embedding parameter. With reference to (5), the nonlinear operator is defined as

$$N[\psi(Y; q)] = (1 - s) \frac{d^2 \psi(Y; q)}{dY^2} + \sqrt{2s} \text{We} \left( \frac{d\psi(Y; q)}{dY} \right) \frac{d^2 \psi(Y; q)}{dY^2} + P. \quad (16)$$

The zero-order deformation equation is defined using  $L$ ,  $h$ ,  $q$  and  $N$  as

$$(1 - q)L[\psi(Y; q) - U_0] = hqN[\psi(Y; q)] \quad (17)$$

along with the boundary equations corresponding to each problem

$$\begin{aligned} \psi(-1; q) &= -\gamma \frac{d\psi(-1; q)}{dY}, \quad \psi(1; q) = \gamma \frac{d\psi(1; q)}{dY} && \text{for the Poiseuille flow,} \\ \psi(-1; q) &= -\gamma \frac{d\psi(-1; q)}{dY}, \quad \psi(1; q) = \gamma \frac{d\psi(1; q)}{dY} + U_w && \text{for the Couette flow.} \end{aligned} \quad (18)$$

When  $q = 0$ , the solution is the initial guess approximation

$$\psi(Y; 0) = U_0 \quad (19)$$

and at  $q = 1$ , the final solution is obtained provided  $h \neq 0$

$$\psi(Y; 1) = U(Y). \quad (20)$$

Thus, it may be observed that as the value of  $q$  grows from 0 to 1,  $\psi(Y; q)$  varies steadily from the initial guess  $U_0$  to the final exact expression  $U(Y)$ . Using Taylor's series,  $\psi(Y; q)$  is expanded in a power series of the embedding parameter  $q$  as shown below

$$\psi(Y; q) = U_0 + \sum_{m=1}^{\infty} U_m(Y) q^m \quad (21)$$

such that

$$U_m(Y) = \frac{1}{m!} \left. \frac{d^m \psi(Y; q)}{dq^m} \right|_{q=0}. \quad (22)$$

Using (21) and (20) and assuming that the series converges for  $q = 1$ , we have

$$U(Y) = U_0(Y) + \sum_{m=1}^{\infty} U_m(Y). \quad (23)$$

The following vectors are defined

$$U_m = \{U_0, U_1, U_2, \dots, U_m\}. \tag{24}$$

Differentiating (17) with respect to  $q$ ,  $m$ -times and then dividing it by  $m!$  and setting  $q = 0$ , the  $m^{\text{th}}$ -order deformation equation is obtained as

$$L[U_m - \chi_m U_{m-1}(Y)] = hR_m(Y). \tag{25}$$

Accordingly, the boundary equations are reduced to

$$\psi(-1; q)_{m-1} = -\gamma \frac{d\psi(-1; q)_{m-1}}{dY}, \quad \psi(1; q) = \gamma \frac{d\psi(1; q)_{m-1}}{dY}. \tag{26}$$

It may be noted that the boundary conditions for both the Poiseuille and Couette flows are now equal as the constant terms are now eliminated. Also

$$R_m(Y) = (1 - s)U''_{m-1} + \sqrt{2s}We \sum_{i=0}^{m-1-i} U_i' U''_{m-1-i} + (1 - \chi_m)P, \tag{27}$$

where

$$\chi_m = \begin{cases} 0 & \text{for } m \leq 1, \\ 1 & \text{for } m > 1. \end{cases} \tag{28}$$

The number of terms in the series solution should be such that the solution converges sufficiently. In order to achieve that the series is convergent sufficiently and quickly, the convergence control parameter has to be chosen carefully. As already defined in the literature [17], the  $q$  values have been narrowed down to the range  $[-2, 0]$ . To get the optimum value of  $q$  in the given range, we check the minimum residual error using the expression [16]

$$E_{U,m} = \frac{1}{K} \sum_{i=0}^K \left[ N \left( \sum_{j=0}^m U_j(i\Delta t) \right) \right]^2, \tag{29}$$

where  $K$  is a positive integer and  $\Delta t = 1/K$ . In the present analysis, the value of  $K$  is taken as 20. Fig. 1 shows the best range of  $h$  values that may be considered for the present analysis. It is apparent that the optimal range for the  $h$  value coincide for both the Poiseuille and Couette flows. Consequently, the optimum value for  $h$  with the least amount of error coincide for both the flows. The  $h$ -values for different order of approximation is shown in Table 1. For the present analysis, the optimum value of  $h$  has been taken as  $-1.32$ .

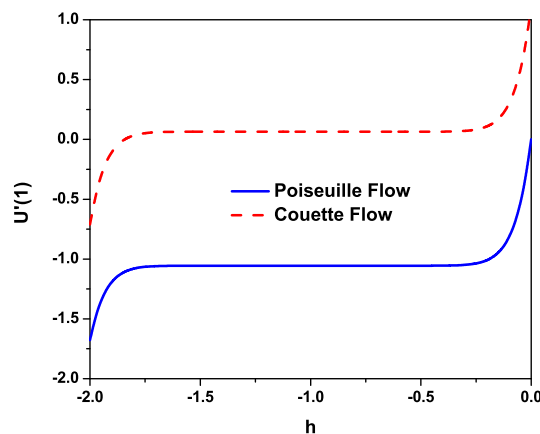


Fig. 1.  $h$  – curve

Table 1.  $h$  values corresponding to the Poiseuille and Couette flows for different approximations

order $m$	Poiseuille flow		Couette flow	
	$h$	minimum error	$h$	minimum error
10	-1.32	$7.34 \times 10^{-18}$	-1.32	$2.82 \times 10^{-18}$
12	-1.32	$5.73 \times 10^{-21}$	-1.32	$1.86 \times 10^{-21}$
15	-1.32	$1.82 \times 10^{-24}$	-1.32	$1.51 \times 10^{-24}$

#### 4. Discussion

From Figs. 2 and 3, we can observe the effect of slip parameter on the velocity profile for both the Poiseuille and Couette flows, respectively. A high value of slip parameter  $\gamma$  indicates that there is a high interaction between the fluid particles and the solid wall. Hence, we can see that an increase in the slip parameter reduces the flow velocity significantly. This is a common phenomenon in flows with the Navier slip and has been discussed at length in the literature [5, 10, 22]. We can see the impact of the dimensionless Weissenberg number on the Poiseuille and Couette flows from Figs. 4 and 5, respectively. The Weissenberg number is the ratio of elastic forces and viscous forces. For both flows, we can see a slight decline in the flow

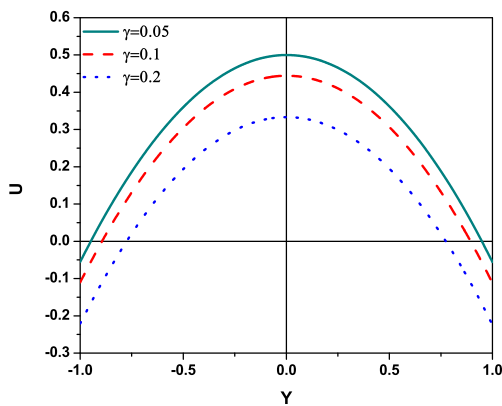


Fig. 2. Poiseuille flow: Effect of slip parameter on velocity

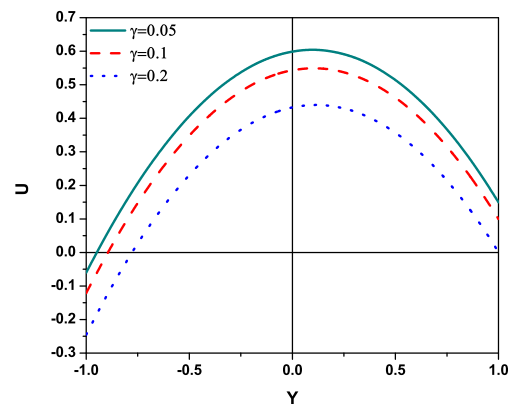


Fig. 3. Couette flow: Effect of slip parameter on velocity

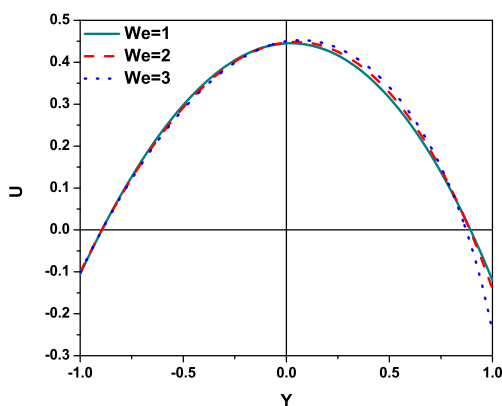


Fig. 4. Poiseuille flow: Effect of Weissenberg number on velocity

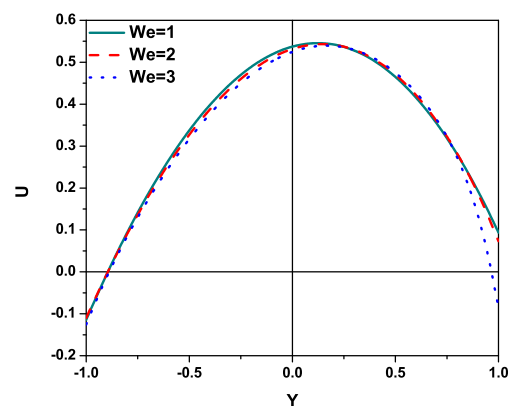


Fig. 5. Couette flow: Effect of Weissenberg number on velocity

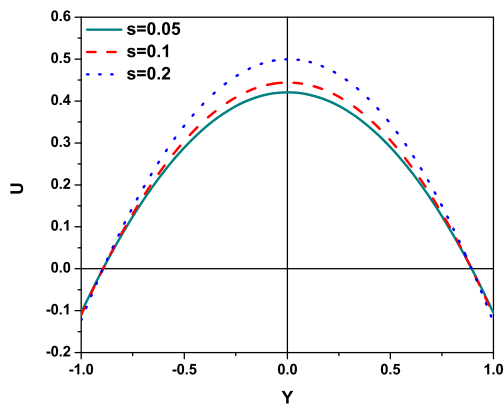


Fig. 6. Poiseuille flow: Effect of power law index on velocity

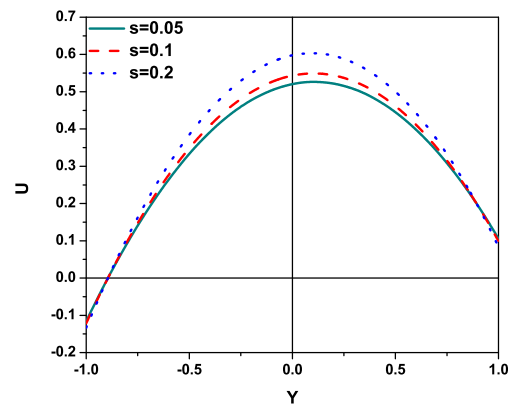


Fig. 7. Couette flow: Effect of power law index on velocity

velocity when the Weissenberg number is increased. However, an increase in velocity is noted in the upper half of the channel with the Weissenberg number. For the flow reversal region near the upper wall in the Poiseuille flow, it can be seen that the flow reversal velocity increases with the Weissenberg number. For the Couette flow, flow reversal was noted near the upper wall of the channel for large Weissenberg number. For Poiseuille flow, the deviation in velocity was greater in the upper half of the channel while it is larger in the lower half of the channel for Couette flow. An increase in the power law index and its influence on the flow velocity of the Poiseuille and Couette flows can be observed from Figs. 6 and 7, respectively. It is apparent that the increase in power law index enhances the flow velocity significantly.

Figs. 8 and 9 display the effect of slip parameter on the skin friction on the lower wall. For the Poiseuille flow, we can see that the increase in slip parameter reduces the skin friction while the skin friction for the Couette flow is increased significantly. However, the reaction of skin friction to the increase in power law index by the Poiseuille and Couette flows is similar as shown in Figs. 10 and 11, respectively. We can see that there is a prominent increase in skin friction when the power law index is increased. The skin friction displayed in Figs. 8–11 are taken as a function of the Weissenberg number. It can be seen that the increase in the Weissenberg number reduces the friction at the wall. This shows that with the dominance of elastic forces over the viscous forces, friction at the walls of the channel may be reduced accordingly.

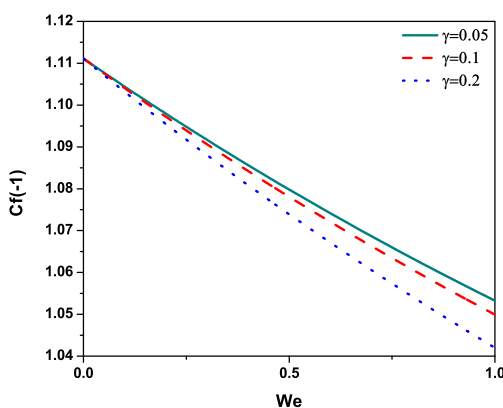


Fig. 8. Poiseuille flow: Effect of slip parameter on skin friction

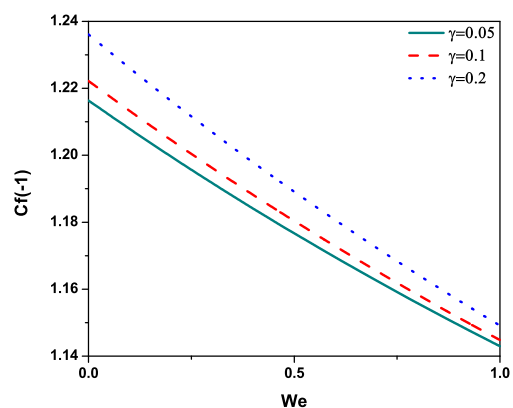


Fig. 9. Couette flow: Effect of slip parameter on skin friction

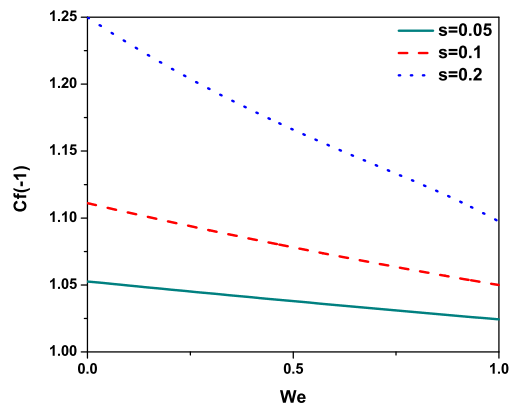


Fig. 10. Poiseuille flow: Effect of power law index on skin friction

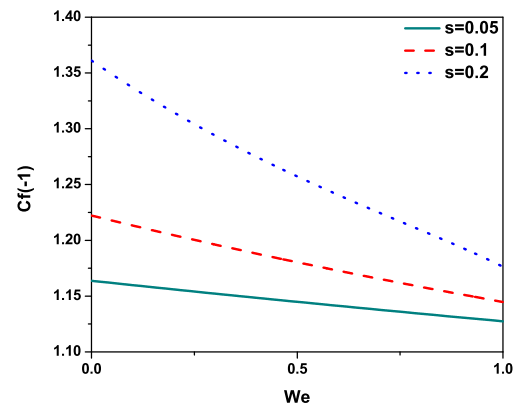


Fig. 11. Couette flow: Effect of power law index on skin friction

## 5. Conclusions

The investigation focused on the Poiseuille and Couette flows of a pressure driven non-Newtonian hyperbolic tangent fluid flow while considering the effect of the Navier slips at the walls. The momentum equation of the flow was reduced to a non-dimensional form after appropriate transformation. The homotopy analysis method was applied to solve the nonlinear second order governing differential equation. The velocity expression was obtained and the effect of pertinent flow parameters for both the Poiseuille and Couette flows was studied and discussed. The increase in value of the power law index significantly enhanced the velocity and skin friction of both flows. However, the effects of varying the value of the Weissenberg number on the velocity and skin friction were not too significant although they were noticeable. As noticed in the case of Newtonian fluids, flow reversal has also been observed in the present investigation. This is caused by the deceleration of flow due to the presence of the Navier slip at the walls [30].

## Acknowledgements

The financial support provided by TEQIP-III, NIT Mizoram is acknowledged.

## References

- [1] Abbasbandy, S., Soliton solutions for the Fitzhugh-Nagumo equation with the homotopy analysis method, *Applied Mathematical Modelling* 32 (12) (2008) 2706–2714. <https://doi.org/10.1016/j.apm.2007.09.019>
- [2] Abbasbandy, S., The application of homotopy analysis method to solve a generalized Hirota-Satsuma coupled KdV equation, *Physics Letters, Section A: General, Atomic and Solid State Physics* 361 (6) (2007) 478–483. <https://doi.org/10.1016/j.physleta.2006.09.105>
- [3] Ali Abbas, M., Bai, Y., Bhatti, M., Rashidi, M., Three dimensional peristaltic flow of hyperbolic tangent fluid in non-uniform channel having flexible walls, *Alexandria Engineering Journal* 55 (1) (2016) 653–662. <https://doi.org/10.1016/j.aej.2015.10.012>
- [4] Atif, S.M., Hussain, S., Sagheer, M., Effect of viscous dissipation and Joule heating on MHD radiative tangent hyperbolic nanofluid with convective and slip conditions, *Journal of the Brazilian Society of Mechanical Sciences and Engineering* 41 (4) (2019) 1–17. <https://doi.org/10.1007/s40430-019-1688-9>

- [5] Aziz, A., Jamshed, W., Aziz, T., Mathematical model for thermal and entropy analysis of thermal solar collectors by using Maxwell nanofluids with slip conditions, thermal radiation and variable thermal conductivity, *Open Physics* 16 (1) (2018) 123–136. <https://doi.org/10.1515/phys-2018-0020>
- [6] Bhattar, S., Mathur, A., Kumar, D., Singh, J., A new analysis of fractional Drinfeld-Sokolov-Wilson model with exponential memory, *Physica A: Statistical Mechanics and its Applications* 537 (2020) 122–136. <https://doi.org/10.1016/j.physa.2019.122578>
- [7] Bhatti, M. M., Yousif, M. A., Mishra, S. R., Shahid, A., Simultaneous influence of thermo-diffusion and diffusion-thermo on non-Newtonian hyperbolic tangent magnetised nanofluid with Hall current through a nonlinear stretching surface, *Pramana – Journal of Physics* 93 (6) (2019) 1–10. <https://doi.org/10.1007/s12043-019-1850-z>
- [8] Devakar, M., Sreenivasu, D., Shankar, B., Analytical solutions of couple stress fluid flows with slip boundary conditions, *Alexandria Engineering Journal* 53 (3) (2014) 723–730. <https://doi.org/10.1016/j.aej.2014.06.005>
- [9] Hashim, I., Abdulaziz, O., Momani, S., Homotopy analysis method for fractional IVPs, *Communications in Nonlinear Science and Numerical Simulation* 14 (3) (2009) 674–684. <https://doi.org/10.1016/j.cnsns.2007.09.014>
- [10] Hasnain, J., Abbas, Z., Aqeel, M., Ghaffari, A., Mustafa, I., Series solution of slip flow of  $Al_2O_3$  and  $Fe_3O_4$  nanoparticles in a horizontal channel with porous medium by using least square and Galerkin methods, *Scientia Iranica* (2019). <https://doi.org/10.24200/sci.2019.52830.2904>
- [11] Hayat, T., Shafique, M., Tanveer, A., Alsaedi, A., Magnetohydrodynamic effects on peristaltic flow of hyperbolic tangent nanofluid with slip conditions and Joule heating in an inclined channel, *International Journal of Heat and Mass Transfer* 102 (2016) 54–63. <https://doi.org/10.1016/j.ijheatmasstransfer.2016.05.105>
- [12] Hayat, T., Shafique, M., Tanveer, A., Alsaedi, A., Radiative peristaltic flow of Jeffrey nanofluid with slip conditions and joule heating, *PLOS ONE* 11 (2) (2016) 1–11. <https://doi.org/10.1371/journal.pone.0148002>
- [13] Hayat, T., Shafique, M., Tanveer, A., Alsaedi, A., Slip and Joule heating effects on radiative peristaltic flow of hyperbolic tangent nanofluid, *International Journal of Heat and Mass Transfer* 112 (2017) 559–567. <https://doi.org/10.1016/j.ijheatmasstransfer.2017.03.116>
- [14] Hussain, A., Malik, M. Y., Salahuddin, T., Rubab, A., Khan, M., Effects of viscous dissipation on MHD tangent hyperbolic fluid over a nonlinear stretching sheet with convective boundary conditions, *Results in Physics* 7 (2017) 3502–3509. <https://doi.org/10.1016/j.rinp.2017.08.026>
- [15] Khan, M., Rasheed, A., Salahuddin, T., Radiation and chemical reactive impact on tangent hyperbolic fluid flow having double stratification, *AIP Advances* 10 (7) (2020) 075 211. <https://doi.org/10.1063/5.0003717>
- [16] Liao, S., An optimal homotopy-analysis approach for strongly nonlinear differential equations, *Communications in Nonlinear Science and Numerical Simulation* 15 (8) (2010) 2003–2016. <https://doi.org/10.1016/j.cnsns.2009.09.002>
- [17] Liao, S., *Beyond perturbation: Homotopy, Modern Mechanics and Mathematics*, volume 2, Chapman and Hall/CRC, 2004.
- [18] Liao, S., On the homotopy analysis method for nonlinear problems, *Applied Mathematics and Computation* 147 (2) (2004) 499–513. [https://doi.org/10.1016/S0096-3003\(02\)00790-7](https://doi.org/10.1016/S0096-3003(02)00790-7)
- [19] Liao, S., Notes on the homotopy analysis method: Some definitions and theorems, *Communications in Nonlinear Science and Numerical Simulation* 14 (4) (2009) 983–997. <https://doi.org/10.1016/j.cnsns.2008.04.013>
- [20] Molabahrami, A., Khani, F., The homotopy analysis method to solve the Burgers-Huxley equation, *Nonlinear Analysis: Real World Applications* 10 (2) (2009) 589–600. <https://doi.org/10.1016/j.nonrwa.2007.10.014>

- [21] Nayak, M., Shaw, S., Makinde, O. D., Chamkha, A. J., Investigation of partial slip and viscous dissipation effects on the radiative tangent hyperbolic nanofluid flow past a vertical permeable Riga plate with internal heating: Bungiorno model, *Journal of Nanofluids* 8 (1) (2019) 51–62. <https://doi.org/10.1166/jon.2019.1576>
- [22] Rashid, M., Khan, M. I., Hayat, T., Khan, M. I., Alsaedi, A., Entropy generation in flow of ferro-magnetic liquid with nonlinear radiation and slip condition, *Journal of Molecular Liquids* 276 (2019) 441–452. <https://doi.org/10.1016/j.molliq.2018.11.148>
- [23] Rashidi, M. M., Domairry, G., Dinarvand, S., Approximate solutions for the Burger and regularized long wave equations by means of the homotopy analysis method, *Communications in Nonlinear Science and Numerical Simulation* 14 (3) (2009) 708–717. <https://doi.org/10.1016/j.cnsns.2007.09.015>
- [24] Sahraoui, M., Kaviany, M., Slip and no-slip velocity boundary conditions at interface of porous, plain media, *International Journal of Heat and Mass Transfer* 35 (4) (1992) 927–943. [https://doi.org/10.1016/0017-9310\(92\)90258-T](https://doi.org/10.1016/0017-9310(92)90258-T)
- [25] Shafiq, A., Hammouch, Z., Sindhu, T. N., Bioconvective MHD flow of tangent hyperbolic nanofluid with newtonian heating, *International Journal of Mechanical Sciences* 133 (2017) 759–766. <https://doi.org/10.1016/j.ijmecsci.2017.07.048>
- [26] Shah, Z., Khan, A., Khan, W., Kamran Alam, M., Islam, S., Kumam, P., Thounthong, P., Micropolar gold blood nanofluid flow and radiative heat transfer between permeable channels, *Computer Methods and Programs in Biomedicine* 186 (2020) 105–197. <https://doi.org/10.1016/j.cmpb.2019.105197>
- [27] Shu, J. J., Teo, J. B. M., Chan, W. K., A new model for fluid velocity slip on a solid surface, *Soft Matter* 12 (2016) 8388–8397. <https://doi.org/10.1039/C6SM01178K>
- [28] Srinivas, J., Murthy, J. V., Chamkha, A. J., Analysis of entropy generation in an inclined channel flow containing two immiscible micropolar fluids using HAM, *International Journal of Numerical Methods for Heat and Fluid Flow* 26 (3–4) (2016) 1027–1049. <https://doi.org/10.1108/HFF-09-2015-0354>
- [29] Tan, Y., Abbasbandy, S., Homotopy analysis method for quadratic Riccati differential equation, *Communications in Nonlinear Science and Numerical Simulation* 13 (3) (2008) 539–546. <https://doi.org/10.1016/j.cnsns.2006.06.006>
- [30] Willert, C., Cuvier, C., Foucaut, J., Klinner, J., Stanislas, M., Laval, J., Srinath, S., Soria, J., Amili, O., Atkinson, C., Kähler, C., Scharnowski, S., Hain, R., Schröder, A., Geisler, R., Agocs, J., Röse, A., Experimental evidence of near-wall reverse flow events in a zero pressure gradient turbulent boundary layer, *Experimental Thermal and Fluid Science* 91 (2018) 320–328. <https://doi.org/10.1016/j.expthermflusci.2017.10.033>
- [31] Yabushita, K., Yamashita, M., Tsuboi, K., An analytic solution of projectile motion with the quadratic resistance law using the homotopy analysis method, *Journal of Physics A: Mathematical and Theoretical* 40 (29) (2007) 8403–8416. <https://doi.org/10.1088/1751-8113/40/29/015>
- [32] Zehra, I., Kousar, N., Rehman, K. U., Pressure dependent viscosity subject to Poiseuille and Couette flows via Tangent hyperbolic model, *Physica A: Statistical Mechanics and its Applications* 527 (2019) 121–332. <https://doi.org/10.1016/j.physa.2019.121332>